Applied Radiation and Isotopes 83 (2014) 100–104

Contents lists available at ScienceDirect

Applied Radiation and Isotopes

journal homepage: www.elsevier.com/locate/apradiso

Multiscale physics of ion-induced radiation damage

Eugene Surdutovich [a], A.V. Solov'yov [b,*]

[a] Physics Department, Oakland University, Rochester, MI 48309, USA
[b] Frankfurt Institute for Advanced Studies, Frankfurt am Main, Germany

HIGHLIGHTS

- The interdisciplinary science of IBCT relates biodamage with physical parameters.
- The multiscale approach is designed for understanding the mechanisms of biodamage.
- Distributions of damage complexity and dose lead to alternative survival curves.
- Thermomechanical mechanism of radiation damage with ions has to be accounted for.
- Studying of germane effects is the key to the quantitative assessment of biodamage.

ARTICLE INFO

Available online 7 February 2013

Keywords:
Radiation damage
Ion-beam therapy
DNA damage
Multiscale approach
Complex DNA damage
Thermomechanical DNA damage

ABSTRACT

This is a review of a multiscale approach to the physics of ion-beam cancer therapy, an approach suggested in order to understand the interplay of a large number of phenomena involved in the radiation damage scenario occurring on a range of temporal, spatial, and energy scales. We describe different effects that take place on different scales and play major roles in the scenario of interaction of ions with tissue. The understanding of these effects allows an assessment of relative biological effectiveness that relates the physical quantities, such as dose, to the biological values, such as the probability of cell survival.

1. Introduction

The scientific interest in obtaining a deeper understanding of radiation damage is motivated by the development of ion-beam cancer therapy and other applications of ions interacting with biological targets. A number of important scientific questions, especially related to DNA damage assessment on the molecular level, have not yet been resolved. Therefore, recently this field has attracted much attention from the scientific community (Surdutovich, 2012; Schardt et al., 2010; Kumar and Sevilla, 2010; Solov'yov et al., 2009). There are a series of conferences devoted to these subjects, such as RADAM (Baccarelli et al., 2010) and later Nano-IBCT (http://nano-ibct.sciencesconf.org/). The latter became possible due to the support of the European framework for Cooperation in Science and Technology (COST). The COST Action, "Nano-scale insights in ion beam cancer therapy (Nano-IBCT)" (http://fias.uni-frankfurt.de/nano-ibct/) was approved in 2010. Among these studies is the multiscale approach to the assessment of radiation damage induced by irradiation with ions. It is aimed at a phenomenon-based quantitative understanding of the scenario from the incidence of an energetic ion on tissue to the cell death. This method combines many spatial, temporal, and energy scales, and is therefore a truly multiscale approach. The variety of these scales and corresponding disciplines is presented in Fig. 1.

The understanding and assessment of radiation damage due to ionizing radiation are at the focus of radiation biophysics, which has a wide scope of important applications from radiation protection to radiation therapy. The standard scope of radiation biophysics spans from the interaction of ionizing projectiles with matter, radiation chemistry that includes interactions of radiation and secondary particles with water and biomolecules, to the analysis of models of cell survival (Alpen, 1998; Lehnert, 2008; Hall and Giaccia, 2012).

One way to address the problem of biological damage starts from the analysis of so-called survival curves. The survival curve is a relation between the logarithm of cell-survival fraction and the deposited dose. These curves can be obtained experimentally and they differ for different species, cells, radiation modality, etc. Nevertheless, the main feature of these curves is that they are approximately parabolic, i.e.,

$$-\ln S/S_0 = \alpha D + \beta D^2, \tag{1}$$

where S/S_0 is the normalized cell survival, D is the dose, and α and β are coefficients. If the dose distribution is uniform, as when

* Corresponding author. Tel.: +49 6979847507.
E-mail address: solovyov@fias.uni-frankfurt.de (A.V. Solov'yov).

0969-8043/$ - see front matter © 2013 Elsevier Ltd. All rights reserved.
http://dx.doi.org/10.1016/j.apradiso.2013.01.035

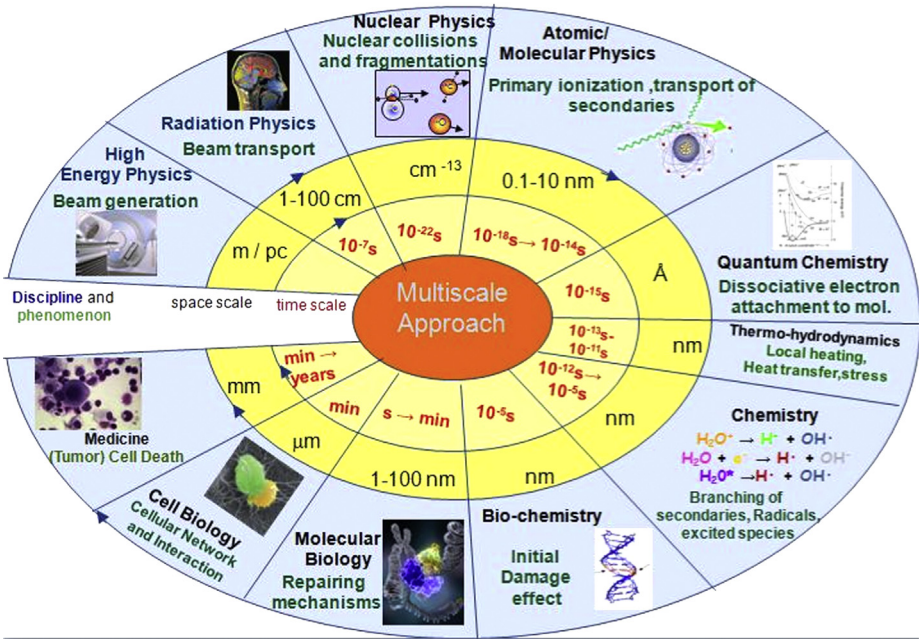

Fig. 1. The variety of temporal and spatial scales corresponding to different aspects and disciplines involved in the science of IBCT.

tissue is irradiated with x-rays, it is possible to find the parameters α and β empirically and use them in treatment planning to determine necessary dose and optimize its delivery.

Particle projectiles change this picture. The dose distribution around each particle's path is highly nonuniform because of the number of secondary electrons released by the ionized molecules of the medium on every nm of the path. These electrons as well as holes and radicals comprise a complicated track structure with a radial distribution of the dose, while the space between different tracks is largely undisturbed. A solution to this problem was suggested by the Katz approach in which the radial dose distribution is calculated and related to the inactivation of sub-cell-nucleus targets (Butts and Katz, 1967; Katz et al., 1971; Cucinotta et al., 1999). The quality factor of radiation was introduced in order to relate the survival curve parameters to a given radiation, differentiating between track types, inactivation modes, the structural complexity of targets, etc. The eventual goal of the Katz model was to calculate the relative biological effectiveness (RBE) (Schardt et al., 2010; Alpen, 1998; Hall and Giaccia, 2012), one of the key integral characteristics of the effect of ions compared to that of photons. This ratio compares the doses of different projectiles leading to the same biological effect. Nevertheless, the biological relation of the radial dose distribution with the cell survival probability was done based on the survival curves for x-rays, without analyzing particular physical processes, i.e., the empiric coefficients α and β remain central to this approach. A desire to understand on a quantitative level what is behind these parameters brought about a multiscale approach to the radiation damage with ions.

The multiscale approach was formulated in Solov'yov et al. (2009) and Surdutovich and Solov'yov (2009), where a scenario leading to DNA damage was suggested. Then, it was further elaborated as different aspects of the scenario were added in a series of works (Surdutovich et al., 2009, 2011; Scifoni et al., 2010a; Toulemonde et al., 2009; Surdutovich and Solov'yov, 2010; Yakubovich et al., 2012). Its name emphasizes the fact that important interactions involved in the scenario happen on a variety of temporal, spatial, and energy scales. Right from the beginning, the approach was formulated as phenomenon-based and was aimed at elucidating the physical, chemical, or biological effects that are important or dominating on each scale in time, space, and energy.

The multiscale approach raised questions about the nature of the effects that take place and lead to survival curves and the calculation of RBE and other macroscopic quantities, i.e. by the end of the day it should answer the question of what is behind the coefficients in Eq. (1). The main issues addressed by the multiscale approach are ion stopping in the medium, the production and transport of secondary electrons produced as a result of ionization and excitation of the medium, the interaction of secondary particles with biological molecules, the most important being DNA, the analysis of induced damage, and the evaluation of the probabilities of subsequent cell survival or death. These effects are happening on time scales ranging from 10^{-21} to 10^{-5} s, i.e., from nuclear to biochemical times. The aim of the physical part of the analysis is the calculation of the spatial distribution of primary DNA damage, including the degree of complexity of this damage.

2. Ion stopping and the Bragg peak

The multiscale approach started with the analysis of ion propagation in a medium. Liquid water was used as the medium because human tissues on the average consist of 75% water. These works (Surdutovich et al., 2009; Scifoni et al., 2010a) resulted in the description of the Bragg peak and the energy spectrum of secondary electrons. The Bragg peak in the stopping power of massive charged particles is obtained using a version of the Bethe–Bloch formula (Bethe, 1930; Bloch, 1933a, 1933b). This formula provides the dependence of the stopping power on the energy of the ion and practically depends on the mean excitation energy. This energy for liquid water is chosen somewhere between 70 and 80 eV (Abril et al., 2011; Pshenichnov et al., 2008). Our approach to this problem was different. We chose to use the singly differentiated (with respect to the secondary electron energy) ionization cross sections of water molecules in the medium as a physical input. These cross sections were taken from experiments (Rudd et al., 1992) with parameters tuned for liquid water (Scifoni et al., 2010a). The parameterizations were

also modified to take into account relativistic effects in the beginning of the ion's path. Even a slight change in cross sections in the entrance channel (plateau region of LET curve) may significantly affect the position of the Bragg peak. Energy loss due to excitation of water molecules has also been included in the calculations (Surdutovich et al., 2009). The effect of charge transfer strongly affects the height of the Bragg peak, since it is proportional to the square of the effective charge of the projectile and the latter decreases as the projectile slows down because of the pick off electrons. Barkas's parameterization (Barkas, 1963) was used for the calculation of the effective charge. The next effect, included in Surdutovich et al. (2009), was the scattering of projectiles that naturally occurs as they propagate in the medium. This causes the spread in longitudinal velocities or the so-called energy straggling. This widens and substantially diminishes the Bragg peak for the beam of projectiles. Another effect on this scale, not yet included in the multiscale approach, is the nuclear fragmentation that happens quite often when projectiles collide with the nuclei of the medium. This effect is deemed to be significant, especially for the calculations of the tail in the stopping power curve beyond the Bragg peak (Pshenichnov et al., 2008). As a consequence, we were able to describe the Bragg peak in good agreement with simulations and experiments (Surdutovich et al., 2009, 2010a; Scifoni et al., 2010a) as shown in Fig. 2.

An important difference of our approach, relying on the singly differentiated ionization cross section, allowed us to not only describe the Bragg peak, but also to use these cross sections too calculate the energy spectrum of secondary electrons, which turned out to be quite useful on the following scale of the electron transport and interactions of electrons with the medium.

A new development has been reported in de Vera et al. (accepted for publication), where a semiempirical model for calculating the electron emission from any organic compound after ion impact was employed in order to extend the calculations to a more realistic medium than liquid water. With the only input of density and composition of the target a quite accurate evaluation of ionization cross sections for such media became possible. Results for protons impacting in the most representative biological targets, such as water or DNA components, were compared well to experimental data. Due to its simplicity and great predictive effectiveness, the method can be immediately extended to any combination of biological target and charged particle of interest in ion beam cancer therapy. As a result, the Bragg peak as well as the energy spectra of secondary electrons can be calculated for more complicated media than liquid water.

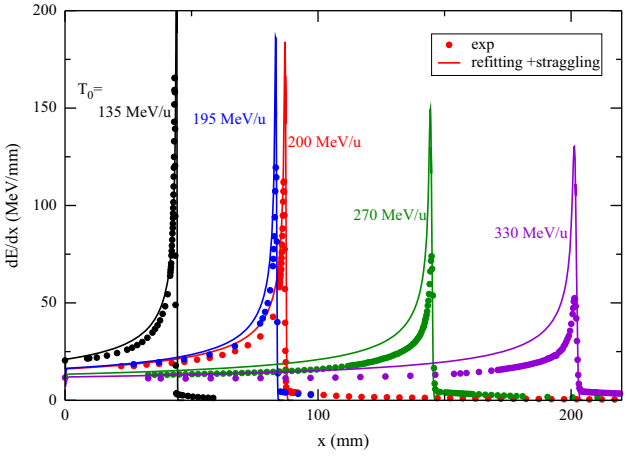

Fig. 2. Linear energy transfer with pronounced Bragg peaks for carbon ions with different initial energies T_0: our model (all lines) compared to experiments from GSI (Haettner et al., 2006) (all dots). Different labels and colors indicate curves at different initial ion-energies T_0 (Scifoni et al., 2010a). (For interpretation of the references to color in this figure caption, the reader is referred to the web version of this article.)

3. Transport of secondary electrons and DNA damage

The next scale in energy and space is related to the transport of the secondary particles, which has been considered in Solov'yov et al. (2009), Scifoni et al. (2010b), Surdutovich et al. (2011), and Surdutovich and Solov'yov (2012a). These papers were built on the inference from the analysis of the energy distribution of secondary electrons that the average energy of these electrons is about 45–50 eV. At these and lower energies, the ionization cross sections are nearly isotropic, which allows one to employ a random walk approximation, i.e., assume that most of secondary electrons (excluding the more energetic δ-electrons) diffuse out from the ion's path. This diffusion was explored in a series of problems. First, we considered a random walk of electrons from the ion's path to a twist of DNA located at some distance from the path (Solov'yov et al., 2009). A single twist of a DNA molecule was chosen because it is an important unit for investigations of double strand breaks (DSBs), significant for the assessment of cell survival. In that study, the number of DSBs per μm of ion's path due to secondary electron action was estimated and compared with biophysical experiments (Tobias et al., 2010).

A later development of that work in Surdutovich et al. (2011) explored a random walk approximation in order to assess the complex DNA damage. Complex DNA damage, investigated by biologists in Ward (1988, 1995), Malyarchuk (2009), and Sage and Harrison (2011), is defined as a multiple number of primary DNA lesions happening on a length of two DNA twists. Such a correlation of lesions is called a cluster with a size equal to the number of singly damaged sites. Different types of lesions may be qualified as effective, e.g., single strand breaks (SSBs), DSBs, base-damages, abasic sites, etc. The size of a cluster is related to the probability of its enzymatic repair. It is deemed that clusters of a sufficiently large size (larger than three or four lesions) are lethal for the cell. Thus, the problem of assessment of complex damage can, on the one hand, be tackled in the same fashion as the problem of DSB, described above; on the other hand, its solution is directly related to the assessment of cell survival as a result of irradiation with ions. The target for a complex damage site is a two-twist segment of a DNA molecule. The original idea for the calculation of complex damage was formulated in Surdutovich et al. (2010b). There, it was suggested that each lesion that counts in a cluster is due to an action of a single agent such as a secondary electron, a radical, etc. Then, if the average number of lesions per target N_i is calculated, the probability of occurrences of clusters of different size, $P_\nu(N_i)$, can be calculated using a Poisson distribution:

$$P_\nu = \exp(-N_i)\frac{N_i^\nu}{\nu!}, \tag{2}$$

where ν is the degree of complexity (Surdutovich et al., 2010b, 2011). The calculation of N_i were solved using the random walk approach (Bug et al., 2012). In that recent work, the random walk calculations were successfully compared with the Monte Carlo simulation of transport of secondary electrons. This comparison is shown in Fig. 3.

The radial distribution of clustered damage sites can be obtained using Eq. (2) and the radial dependence of N_i. Given that damage clusters with degree of complexity exceeding a certain number are lethal (this information comes from the biologists, Sage and Harrison, 2011), we can obtain the radial distribution of cell survival. Independently, the radial dose

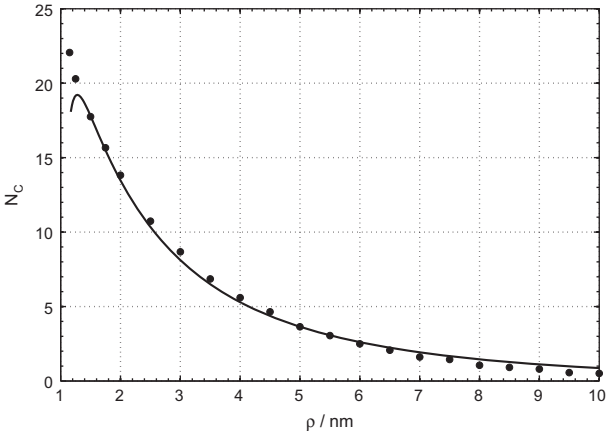

Fig. 3. The fluence of secondary electrons, produced by a carbon ion in the vicinity of the Bragg peak, on a cylinder representing a DNA twist: the random walk calculations (solid line) are compared to the Monte Carlo simulations (Bug et al., 2012).

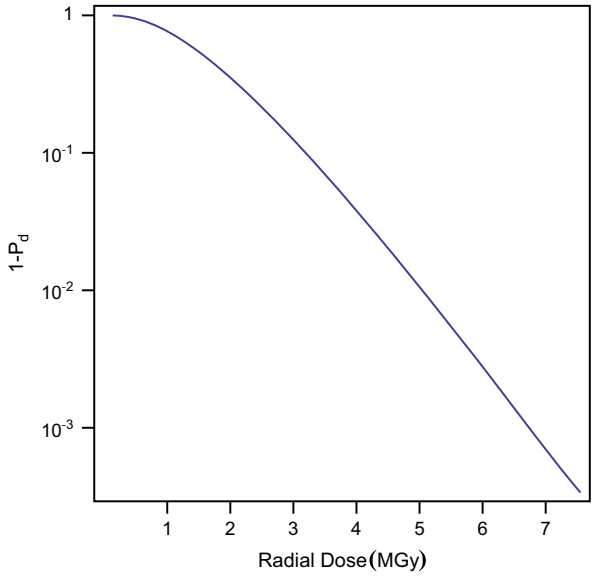

Fig. 4. The dependence of cell survival based on the DNA damage complexity on radial dose (Surdutovich et al., 2011).

distribution around the ion's path can also be calculated using the random walk approach (Surdutovich and Solov'yov, 2012b). Then, the survival curve can be obtained as a parametric plot of cell survival on the radial dose as shown in Fig. 4 (Surdutovich et al., 2011). This is an example of how the multiscale approach can be used for assessment of radiation damage. The involved quantities, the cell survival and the radial dose, are calculated independently based on either physical or biological effects. Their dependence is thus obtained phenomenologically rather than empirically.

4. Local heating and its consequences

Thermomechanical effects stem from the highly inhomogeneous dose deposition by ions. The ions lose most of their energy in the processes of ionization and excitation of the molecules of the medium. As a result a large number of electrons and holes are produced in the vicinity of the ion's path. These processes happen within 10^{-16} s. The electrons lose their energies in cascades of collisions and thermalize by about 10^{-15}–10^{-14} s. At this time they transfer their energy to the molecules. The energy in the latter is distributed between vibrational and translational degrees of freedom and by 10^{-14}–10^{-13} s the medium in the vicinity of the ion's trajectory becomes very hot. The inelastic thermal spike model predicts the temperature increases to be above 1000 K (Toulemonde et al., 2009) for carbon ions in liquid water. Consequently, the pressure above 10 GPa is expected within a cylinder of 1 nm around the ion's path. This pressure initiates a cylindrical shock wave that starts at about 10^{-13} s after the ion's passage (Surdutovich and Solov'yov, 2010).

The pressure in the front of the shock wave gradually decreases with time. A simplified hydrodynamical treatment (Surdutovich and Solov'yov, 2010) predicted the propagation of these waves until 1 ns after the ion's passage. During this time, the wave front propagates for over 90 nm. In reality, the shock waves lose their strength sooner (Yakubovich et al., 2012), but still their effects are expected at distances over 10 nm even for carbon ions. In relation to the radiation damage, we are interested in two effects. The first is the rapid increase of pressure in the wave front with a consequent sharp decrease in the wake of the wave (Surdutovich and Solov'yov, 2010). The second effect is the mass flow transferred by the shock wave.

The pressure on the wavefront is given by (Surdutovich and Solov'yov, 2010)

$$P(t)=\frac{2}{\gamma+1}\rho u_f^2=\frac{\beta^2}{2(\gamma+1)}\frac{\sqrt{\epsilon\rho}}{t}, \tag{3}$$

where t is the time after the ion's traverse, $\gamma=C_P/C_V$ for the medium, u_f is the speed of the wave front, $\beta=0.863$ is a dimensionless constant related to the geometry of the problem (see Surdutovich and Solov'yov, 2010 for more detail), $\rho=1\ \mathrm{g\ cm^{-3}}$ (for liquid water) is the density of the medium, and ϵ is the fraction of the linear energy transfer (LET) that is carried by the shock wave. The radius, R, of the wave front is given by (Surdutovich and Solov'yov, 2010)

$$R(t)=\beta\sqrt{t}\left[\frac{\epsilon}{\rho}\right]^{1/4}. \tag{4}$$

From Eqs. (3) and (4) we can obtain the dependence of pressure on the radius of the wave front:

$$P=\frac{\beta^4}{2(\gamma+1)}\frac{\epsilon}{R^2}. \tag{5}$$

If a biomolecule, such as DNA, appears to be in the vicinity of the ion's path, forces proportional to the above pressure will act on its parts. These forces can be strong enough to break covalent bonds in the backbone of the DNA and thus contribute to the radiation damage. The question of whether the short-time action of such forces is sufficient to cause DNA strand breaks was analyzed in Yakubovich et al. (2012) and Surdutovich et al. (2013) using a Molecular Dynamics (MD) simulation of a shock wave propagating through a nucleosome. At small values of LET, the shock waves are not sufficiently strong and the radiation damage is due to chemical effects such as interaction of DNA molecules with free or solvated electrons, free radicals, holes, etc. In Surdutovich et al. (2013), it is shown that for the bonds located about 2 nm from the ion's path, the critical value of LET at which the direct bond breaking by the shock wave starts to dominate over chemical effects is 5 keV/nm. Eq. (5) tells us that the same (pressure) forces are achieved for the constant ratio of ϵ/R^2. This allows us to calculate the radius of dominance of the direct damage by shock waves (Surdutovich et al., 2013). A LET of about 5 keV/nm is achieved for Ar ions in the vicinity of the Bragg peak. The value of LET is proportional to the square of the effective charge of the ion. This means that when the radiation damage is assessed for ions heavier than Ar, the direct effect has to be taken into account.

5. Conclusion

The main difference of the multiscale approach to the radiation damage from other methods of assessment of radiation damage is the in-depth focusing on physical effects. The main advantages of the multiscale approach follow from its architecture and are its fundamentality and versatility. The approach evaluates the relative contributions and significance of a variety of phenomena; it elucidates a complex multiscale scenario in sufficient detail and has a solid predictive power. It is structurally simple and inclusive, and allows for modifications and extensions by including new effects on different scales and improvements on the way.

The examples of the calculation of the survival curve on the basis of independent calculation of DNA damage complexity and the radial dose and direct thermomechanical damage of DNA molecules by shock waves demonstrate the advantages of the multiscale approach. These examples are still incomplete and more research is needed to make the multiscale approach a worthwhile practical tool for the assessment of radiation damage on the molecular level.

References

Abril, I., Garcia-Molina, R., Denton, C., Kyriakou, I., Emfietzoglou, D., 2011. Radiat. Res. 175, 247–255.

Alpen, E.L., 1998. Radiation Biophysics. Academic Press, San Diego, London, Boston, New York, Sydney, Tokyo, Toronto.

Baccarelli, I., Gianturco, F., Scifoni, E., Solov'yov, A., Surdutovich, E., 2010. Eur. Phys. J. D 60.

Barkas, W.H., 1963. Nuclear Research Emulsions I. Techniques and Theory, vol. 1. Academic Press, New York, London.

Bethe, H., 1930. Ann. Phys. 397, 325–400.

Bloch, F., 1933a. Z. Phys. A: Hadrons Nucl. 81, 363–376.

Bloch, F., 1933b. Ann. Phys. 408, 285–320.

Bug, M., Surdutovich, E., Rabus, H., Rosenfeld, A.B., Solov'yov, A.V., 2012. Eur. Phys. J. D 66, 291.

Butts, J.J., Katz, R., 1967. Radiat. Res. 30, 855–871.

Cucinotta, F., Nikjoo, H., Goodhead, D., 1999. Radiat. Environ. Biophys. 38, 81–92.

de Vera, P., Garcia-Molina, R., Abril, I., Solov'yov, A.V., Phys. Rev. Lett., accepted for publication.

Haettner, E., Iwase, H., Schardt, D., 2006. Radiat. Prot. Dosimetry 122, 485.

Hall, E.J., Giaccia, A.J., 2012. Radiobiology for Radiologist. Lippincott Williams & Wilkins, Philadelphia, Baltimore, New York, London.

〈http://fias.uni-frankfurt.de/nano-ibct/〉.

〈http://nano-ibct.sciencesconf.org/〉.

Katz, R., Ackerson, B., Homayoonfar, M., Sharma, S.C., 1971. Radiat. Res. 47, 402–405.

Kumar, A., Sevilla, M., 2010. Chem. Rev. 110, 7002–7023.

Lehnert, S., 2008. Biomolecular Action of Ionizing Radiation. Taylor & Francis, New York, London.

Malyarchuk, S., Castore, R., Harrison, L., 2009. DNA Repair 8, 1343–1354.

Pshenichnov, I., Mishustin, I., Greiner, W., 2008. Nucl. Instrum. Methods B 266, 1094–1098.

Rudd, M.E., Kim, Y.-K., Madison, D.H., Gay, T., 1992. Rev. Mod. Phys. 64, 441.

Sage, E., Harrison, L., 2011. Mutat. Res. 711, 123–133.

Schardt, D., Elsässer, T., Schulz-Ertner, D., 2010. Rev. Mod. Phys. 82, 383–425.

Scifoni, E., Surdutovich, E., Solovyov, A., 2010a. Phys. Rev. E 81, 021903.

Scifoni, E., Surdutovich, E., Solov'yov, A., 2010b. Eur. Phys. J. D 60, 115.

Solov'yov, A., Surdutovich, E., Scifoni, E., Mishustin, I., Greiner, W., 2009. Phys. Rev. E 79, 011909.

Surdutovich, E., 2012. A. Solov'yov. J. Phys.: Conf. Ser. 373, 012001.

Surdutovich, E., Solov'yov, A., 2009. Europhys. News 40 (2), 21.

Surdutovich, E., Solov'yov, A., 2010. Phys. Rev. E 82, 051915.

Surdutovich, E., Solov'yov, A.V., 2012a. Eur. Phys. J. D 66, 206.

Surdutovich, E., Solov'yov, A.V., 2012b. Eur. Phys. J. D 66, 245.

Surdutovich, E., Obolensky, O., Scifoni, E., Pshenichnov, I., Mishustin, I., Solov'yov, A., Greiner, W., 2009. Eur. Phys. J. D 51, 63–71.

Surdutovich, E., Scifoni, E., Solov'yov, A., 2010a. Mutat. Res. 704, 206–212.

Surdutovich, E., Yakubovich, A., Solov'yov, A., 2010b. Eur. Phys. J. D 60, 101.

Surdutovich, E., Gallagher, D.C., Solov'yov, A.V., 2011. Phys. Rev. E 84, 051918.

Surdutovich, E., Yakubovich, A.V., Solov'yov, A.V., 2013. Sci. Rep. 3, 1289.

Tobias, F., Durante, M., Taucher-Scholz, G., Jakob, B., 2010. Mutat. Res. 704, 54–60.

Toulemonde, M., Surdutovich, E., Solov'yov, A., 2009. Phys. Rev. E 80, 031913.

Ward, J., 1988. Prog. Nucl. Acid. Res. Mol. biol. 35, 95–125.

Ward, J., 1995. Radiat. Res. 142, 362–368.

Yakubovich, A.V., Surdutovich, E., Solov'yov, A.V., 2012. Nucl. Instrum. Method B 279, 135–139.